Anal Bioanal Chem (2008) 392:65–76
DOI 10.1007/s00216-008-2126-5

ORIGINAL PAPER

Attenuated total reflection micro FTIR characterisation of pigment–binder interaction in reconstructed paint films

R. Mazzeo · S. Prati · M. Quaranta · E. Joseph · E. Kendix · M. Galeotti

Received: 1 January 2008 / Revised: 2 April 2008 / Accepted: 10 April 2008 / Published online: 3 May 2008

Abstract The interaction of pigments and binding media may result in the production of metal soaps on the surface of paintings which modifies their visible appearance and state of conservation. To characterise more fully the metal soaps found on paintings, several historically accurate oil and egg yolk tempera paint reconstructions made with different pigments and naturally aged for 10 years were submitted to attenuated total reflectance Fourier transform infrared (ATR FTIR) microspectroscopic analyses. Standard metal palmitates were synthesised and their ATR spectra recorded in order to help the identification of metal soaps. Among the different lead-based pigments, red lead and litharge seemed to produce a larger amount of carboxylates compared with lead white, Naples yellow and lead tin yellow paints. Oil and egg tempera litharge and red lead paints appeared to be degraded into lead carbonate, a phenomenon which has been observed for the first time. The formation of metal soaps was confirmed on both oil and egg tempera paints based on zinc, manganese and copper and in particular on azurite paints. ATR mapping analyses showed how the areas where copper carboxylates were present coincided with those in which azurite was converted into malachite. Furthermore, the key role played by manganese in the production of metals soaps on burnt and raw sienna and burnt and raw umber paints has been observed for the first time. The formation of copper, lead, manganese, cadmium and zinc metal soaps was also identified on egg tempera paint reconstructions even though, in this case, the overlapping of the spectral region of the amide II band with that of metal carboxylates made their identification difficult.

Keywords Metal soaps · Binding media · Oil binder · Egg tempera binder · Micro ATR FTIR · Paintings

R. Mazzeo (✉) · S. Prati · E. Joseph · E. Kendix
Microchemistry and Microscopy Art Diagnostic Laboratory,
University of Bologna,
Via Tombesi dall'Ova 55,
48100 Ravenna, Italy
e-mail: rocco.mazzeo@unibo.it

M. Quaranta
Department of Cultural Heritage, University of Iasi,
700511 Iasi, Romania

M. Galeotti
Laboratorio Scientifico, Opificio delle Pietre Dure,
Via Alfani, 78,
50125 Firenze, Italy

Introduction

Several papers have been published on the interaction between metal salts, present as driers or pigments in painted artworks, and organic binding media with particular reference to drying oils. At the same time the degree to which these interactions affect the analytical detection of linseed oil has been evaluated [1–3] as well as the role played by pigments in the ageing processes of paintings [4]. Moreover research studies aimed at evaluating the degree of hydrolysis induced by different pigments were performed through the analysis of the leachable fraction extracted from naturally aged oil paint layers [1]. Gas chromatographic studies have also underlined how shorter-chain fatty acids, such as acetic and oxalic acids, aldehydes and diacids, are produced as a result of ageing processes [5].

Infrared spectroscopy was used to study the effects of pigments on the ageing of drying oil [4] and the results led to the identification of a triglyceride hydrolysis process

which takes place in the presence of particular pigments such as lead and zinc white. The reduction in the intensity of the ester peak detected in the recorded infrared spectra and the contemporary formation of metal carboxylates were used as the main indicators of the above mentioned deterioration process. While several papers have been already published on the formation of lead, copper and zinc carboxylates [6–14], research on other types of metal carboxylates has been so far neglected.

These saponification processes have important consequences on both the visible appearance and the state of conservation of paintings. In fact, as the saponification progresses paintings appear darker due to the gradual loss of the pigment hiding power. Especially in fresh lead white paints the light is scattered, whereas it is absorbed as the lead soap formation progresses. Environmental humidity plays a crucial role in the hydrolysis of fatty esters which leads to the formation of more hydrophilic and soluble compounds sometimes in the form of surface protrusions [6–9, 11, 12] comprising metal soap aggregates that, by causing expansion, result in the breaking up of the paint layer [10]. In this context, the term "lead white phenomenon" has been known since 1940 and refers to the slightly cracked and mottled appearance of paint oil films with lead-based pigments [13].

Furthermore, metal carboxylates have been detected on the surfaces of metal objects as a result of degradation reactions between the metal body and surface treatments based on the use of drying oil and in contact with other types of organic substrates such as leather [6, 15].

This paper presents the analytical results achieved on the chemical characterisation of the interactions between pigments and binding media carried out by attenuated total reflectance (ATR) microspectroscopy measurements performed non destructively on the surface of historically accurate reconstructions of oil and egg yolk painting composites naturally aged for 10 years. The reconstructions were prepared 10 years ago to provide conservation scientists and conservator-restorers with reference materials and standards for instrumental analysis and visual examinations [16].

ATR analyses showed that all paint reconstructions have been affected by a certain degree of hydrolysis or metal carboxylate formation. In order to facilitate their identification, several metal carboxylates have been synthesised and their specific ATR-FTIR spectra recorded.

The research also allowed the characterisation of a particular degradation effect which took place on the oil azurite paint reconstruction where the pigment itself has been converted into green malachite in the same area in which carboxylates were produced. At the same time the degradation of some lead oxide paints into lead carbonate has been detected.

Materials and methods

Synthesis of standard metal palmitates

It is already known that soaps obtained from different fatty acids with the same metal ion show differences in the spectral range 1000–1300 cm^{-1} where alkyl lateral chains absorb. On the other hand soaps obtained with the same fatty acid but with different metal ions can be identified owing to their different COO^- bands [6]. Due to the fact that within each single paint reconstruction mixtures of carboxylates of the same metal are present, their single characterisation is not possible. For this reason only lead, cobalt, zinc, cadmium and manganese palmitates have been synthesised. Lead and cobalt palmitate were synthesised according to methods reported elsewhere [9, 17]. Lead palmitate was prepared by mixing 30 mL of a 0.02 M solution of lead nitrate [$Pb(NO_3)_2$] (water, ethanol, methanol 5:5:2) with 12.5 mL of a 0.02 M solution of palmitic acid in methanol and leaving the mixture container for 10 min in an ultrasonic bath. The obtained crystallised solid was filtered, washed with ethanol and ether and then vacuum-dried. Cobalt palmitate was prepared by dropwise addition of 2.5 mL of a 0.4 M solution of cobalt acetate [$Co(CH_3COO)_2{\cdot}4H_2O$] to 6 mL of a 0.3 M solution of palmitic acid under stirring, which was maintained for 2 h. The blue precipitate was filtered and vacuum-dried.

A preparation method slightly different from that used to synthesise lead palmitate [9] was adopted for the preparation of zinc, manganese and cadmium palmitates. Cadmium and zinc palmitates were prepared by dropwise addition of 3 mL of a 0.3 M water solution of cadmium acetate [$Cd(CH_3COO)_2{\cdot}2H_2O$] and zinc acetate [$Zn(CH_3COO)_2{\cdot}2H_2O$], respectively, to 12 mL of a 0.2 M solution of palmitic acid in ethanol and the solutions were left at 50 °C for 3 h. The precipitate were then filtered and vacuum-dried.

Manganese(II) and (III) palmitates were prepared by dropwise addition of 3 mL of a 0.4 M water solution of Mn^{II} acetate [$Mn(CH_3COO)_2$] and Mn^{III} acetate [$Mn(CH_3COO)_3{\cdot}3H_2O$], respectively, to 12 mL of a 0.25 M ethanol solution of palmitic acid. A precipitate is formed immediately for Mn^{II}, whereas for Mn^{III} the precipitation of the carboxylate was obtained by leaving the solution for 1 h in an oven at 50 °C. Both precipitates were then filtered and vacuum-dried before recording their infrared spectra.

The copper palmitate was kindly provided by The Canadian Conservation Institute [6].

Paint reconstructions

Historically accurate reconstructions of oil and egg yolk painting composites made by mixing different types of

pigments (Table 1) and binding media were prepared in 1996 by the conservator-restorers of the Opificio delle Pietre Dure in Florence following the ancient Cennino Cennini's paint recipes [18]. The paint reconstructions have been stored within a closed metal cabinet at ambient (laboratory) environmental conditions [16].

Paint reconstructions (Fig. 1) were prepared by applying pigments and binding media on wooden bars preliminarily ground with a mixture of a rabbit glue water solution (1:16) saturated with gypsum.

Two parts yolk, one part egg white and one part vinegar were mixed with pigments to obtain the egg tempera paint reconstructions, whereas standard linseed oil was used as binder for the oil paints. Two films made of only linseed oil and egg tempera binders were applied over the wooden bars in order to be used as reference materials.

Table 1 List of pigments employed in the paint film reconstructions

Colour	Name	Chemical composition[a]	Oil paint	Egg tempera paint
Blue	Azurite	$2CuCO_3{\cdot}Cu(OH)_2$	X	X
	Indigo	$C_{16}H_{10}O_2N_2$	X	
	Lapislazuli	$3Na_2O{\cdot}3Al_2O_3{\cdot}6SiO_2{\cdot}2Na_2S$	X	X
	Cobalt blue	$CoO{\cdot}Al_2O_3$	X	X
	Prussian blue	$Fe_4[Fe(CN)_6]_3$	X	
	Artificial ultramarine	$Na_{8-10}Al_6Si_6O_{29}S_{2-4}$	X	X
	Cerulean blue	$CoO{\cdot}SnO_2$	X	
Red	Cadmium red	$CdS{\cdot}CdSe$	X	
	Red lead	Pb_3O_4	X	X
	Carmine	$C_{21}H_{20}O_{13}$	X	
	Madder	$C_{14}H_8O_4$ +$C_{14}H_8O_5$	X	
	Burnt sienna	Silicate, $Fe_2O_3{\cdot}nH_2O$ + Al_2O_3(60%) + MnO_2(1%)	X	
	Bole	$Al_2O_3{\cdot}SiO_2$+Fe_2O_3	X	X
	Red ochre	Fe oxide, silicate	X	
	Burnt umber	Silicate + $Fe_2O_3MnO_2{\cdot}nH_2O$ + Al_2O_3	X	X
	Raw umber	$Fe_2O_3{\cdot}MnO_2{\cdot}nH_2O$ + silicate + Al_2O_3	X	X
Yellow	Naples yellow	$Pb_3[SbO_4]_2$	X	X
	Litharge	PbO	X	X
	Cadmium yellow	CdS	X	X
	Orpiment	As_2S_3	X	X
	Lead tin yellow	Pb_2SnO_4 or $PbSn_2SiO_7$	X	X
	Realgar	As_2S_2	X	X
	Raw sienna	$Fe_2O_3{\cdot}nH_2O$ + MnO_2+ Al_2O_3+ $SiO_{2x}{\cdot}2H_2O$	X	X
	Yellow ochre	$Fe(OH)_3$	X	X
	Mars yellow	$Fe(OH)_3$+$Al(OH)_3$+$CaSO_4{\cdot}nH_2O$	X	X
	Indian yellow	Mg $C_{19}H_{16}MgO_{11}{\cdot}6H_2O$	X	X
Green	Malachite	$CuCO_3{\cdot}Cu(OH)_2$	X	X
	Green earth	Glauconite celadonite (Fe^{II}, Mg, K silicon aluminate)	X	
	Cobalt green	CoO, ZnO	X	X
	Chrome oxide	Cr_2O_3	X	X
	Emerald green	$Cr_2O(OH)_4$	X	X
	Veronese green	$Cu_3(AsO_4)_2{\cdot}4H_2O$	X	
White	Lead white	$PbCO_3{\cdot}Pb(OH)_2$	X	X
	Zinc white	ZnO	X	X
	Titanium white	TiO_2	X	X
	Chalk	$CaCO_3$	X	X
Black	Ivory black	$Ca_3(PO_4)_2$+$CaCO_3$+carbon	X	
	Vine black	Amorphous carbon	X	
	Lamp black	Amorphous carbon	X	
Grey	Bone black + lead white	$Ca_3(PO_4)_2$+$CaCO_3$+C+$PbCO_3{\cdot}Pb(OH)_2$	X	
	Vine black + lead white	Amorphous carbon+$PbCO_3{\cdot}Pb(OH)_2$	X	
	Lamp black + lead white	Amorphous carbon+$PbCO_3{\cdot}Pb(OH)_2$	X	

[a] Chemical composition as reported into the pigments' specification sheet provided by the Zecchi company (www.zecchi.it, Florence, Italy) from where pigments were purchased

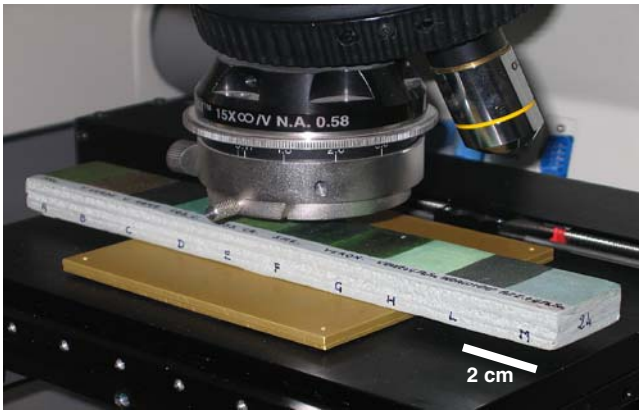

Fig. 1 A wooden bar containing a paint reconstruction positioned on the FTIR motorised microscope stage ready for analysis by the micro slide-on ATR crystal connected to a 15× objective

Micro ATR spectroscopic analysis

Micro ATR analyses were performed non destructively, without any type of preparation, by just positioning the powder carboxylates or the paint reconstructions onto the FTIR microscope *xyz* motorised stage (Fig. 1). ATR spectra were acquired in the range 4000–650 cm^{-1} with a Thermo-Nicolet Nexus 5700 spectrometer connected to a Thermo Continuum IR microscope, fitted with an MCT type A detector cooled by liquid nitrogen. Measurements were made with the microscope in reflection mode, using a 15× Thermo-Electron Infinity Reflachromat objective and a tube factor of 10×. A micro slide-on ATR with a silicon crystal (contact area diameter 120 μm) was connected to the 15× objective. Single-point ATR measurements (a minimum of three) were performed on the surface of each paint reconstruction by recording a total of 64 scans and averaging the resulting interferogram, with a resolution of 4 cm^{-1}. ATR mapping was also performed on selected areas. Once a spatially related series of spectra have been acquired a data processing method, using Nicolet "Omnic-Atlμs" software, treat the set of spectra collectively i.e. the whole data set were baseline-corrected rather than each spectrum having to be processed individually. Then, specific chemical absorption bands of the compound under investigation were selected and their areas plotted against the spatial position of each spectrum in the series. This approach allowed information on the spatial distribution of the identified chemical compounds. A total of 72 spectra

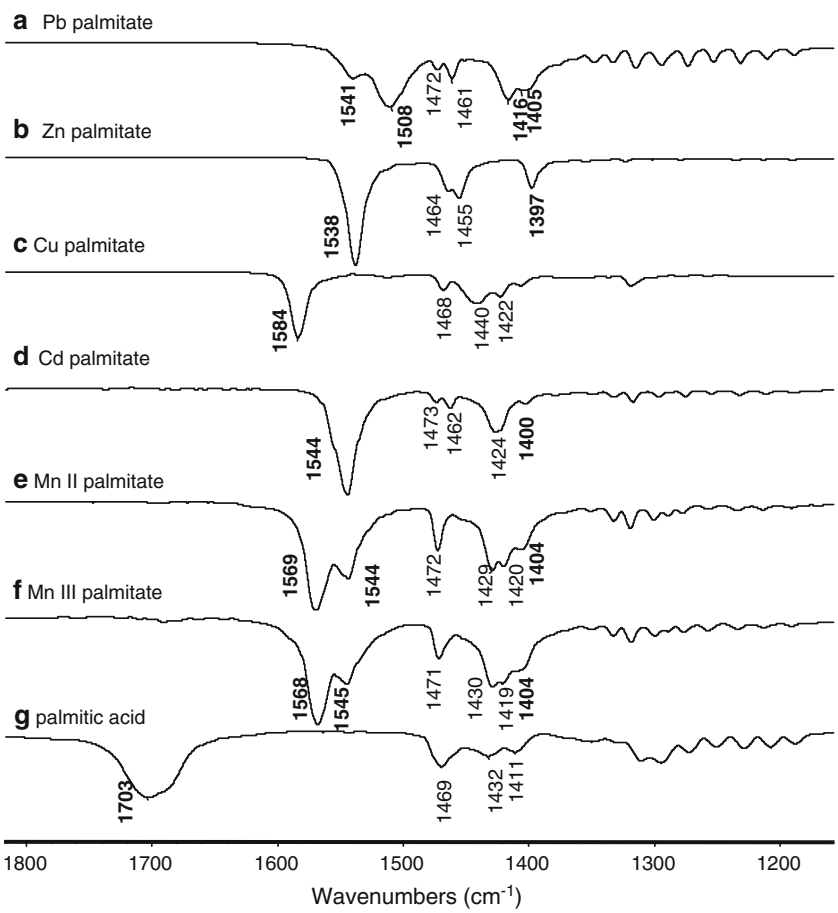

Fig. 2 ATR spectra of **a** lead palmitate, **b** zinc palmitate, **c** copper palmitate, **d** cadmium palmitate, **e** Mn(II) palmitate, **f** Mn(III) palmitate and **g** palmitic acid. The characteristic absorption bands of carboxylates are highlighted in *bold*

were collected with a step size of 20 μm. Each false colour image obtained from the map data set results from the area of one specific chemical vibration band (chemical map) plotted against the spatial position of each spectrum in the data set.

Results and discussion

Analyses of standard metal palmitates

The ATR spectra of the synthesised metal palmitates (Pb, Zn, Cu, Cd, Mn^{II} and Mn^{III}) obtained from the reaction with palmitic acid are shown in Fig. 2. All metal palmitates present characteristic absorption bands in the spectral region between 1600 and 1400 cm^{-1} where the asymmetric and symmetric stretching vibrations of the COO^- group occur. The spectrum of lead palmitate (Fig. 2a) shows two characteristic bands at 1508 and 1541 cm^{-1}, the former showing a stronger intensity. Spectra of zinc, copper and cadmium palmitates (Fig. 2b–d) show just one absorption band at 1538, 1584 and 1544 cm^{-1}, respectively. The Mn^{II} and Mn^{III} palmitates (Fig. 2e,f) show similar spectra profiles and are characterised by a strong band at 1568 cm^{-1} and a weaker band at 1545 cm^{-1}. All spectra show that there is no trace left of unreacted free palmitic acid (Fig. 1g), since absorption band at 1703 cm^{-1} is absent. All these bands have been used as reference values in the identification of metal carboxylates possibly produced on the surface of the paint reconstructions.

Reference oil and egg tempera films

Figure 3 reports the ATR spectra of pure stand linseed oil (Fig. 3a) and egg tempera (Fig. 3b) films naturally aged for 10 years; Table 2 lists the assignment of vibrational frequencies to chemical fragments. Linseed oil shows a broad band at 3440 cm^{-1} which is generally assigned to the stretching of alcohol and hydroperoxide bonds formed as a result of the polymerisation and ageing processes occurring in the oil film during which the double bonds present in the triglyceride moieties undergo oxidation [19]. With ageing the ester stretching band at about 1735 cm^{-1} becomes broader [4] as a result of the hydrolysis of triglycerides and the formation of other degradation products such as aldehydes, ketones, anhydrides, lactones and free fatty acids, which can be detected trough the appearance of a distinctive absorption band at 1711 cm^{-1}.

It is known that ageing of egg tempera paints mainly affects the triglycerides component, while changes occurring at the level of proteinaceous components are still unknown. In particular the degree of unsaturation, which is largely lower than in siccative oil, is further reduced and the intensity of the ester band decreases, with the formation of free fatty acids groups being indicative of a partial hydrolysis of the triglycerides [20].

The two strong absorption bands at around 1650 cm^{-1} (amide I) and 1550 cm^{-1} (amide II) (Fig. 3b) are typical protein bands which are mainly attributed to the C=O stretching and N–H bending vibrations, respectively, of amide groups of the peptide backbone in proteins.

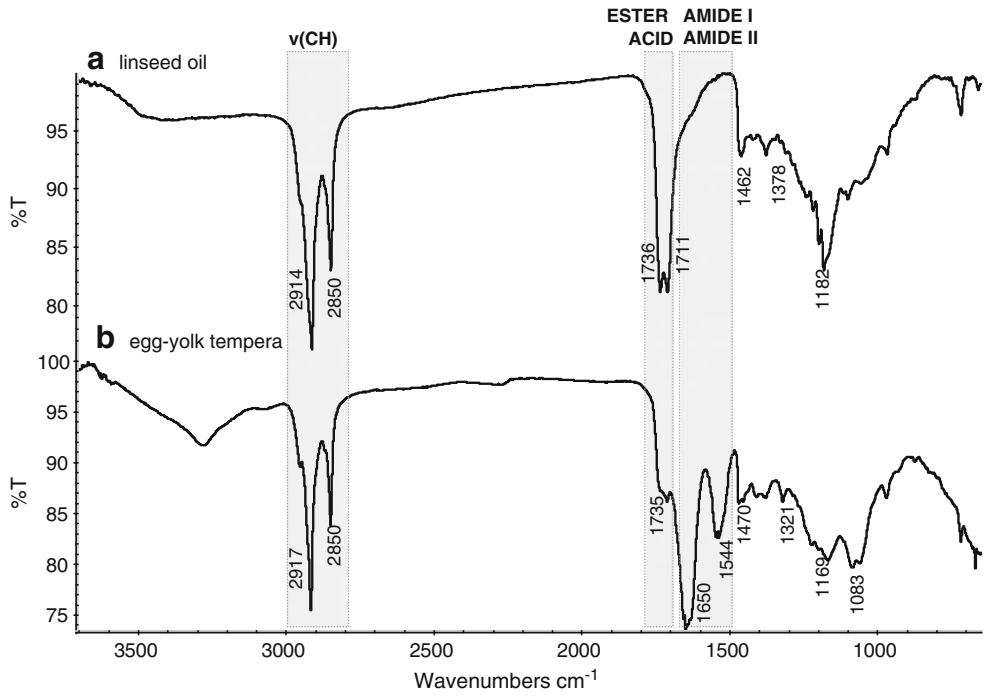

Fig. 3 ATR spectra of films of **a** stand linseed oil and **b** egg yolk tempera aged naturally for 10 years

Table 2 ATR infrared absorptions bands characteristic of 10-year-old linseed oil and egg tempera films

Linseed oil (cm^{-1})	Egg tempera (cm^{-1})	Assignment
3440 w		O–H stretching
	3288 m	N–H stretching
	3080 w	Amide II overtone
2955 sh	2955 w	$\nu_{AS}CH_3$ stretching
2920 vs	2920 vs	$\nu_{AS}CH_2$ stretching
2870 sh	2870 w	$\nu_{S}CH_3$ stretching
2850 s	2850 s	$\nu_{S}CH_2$ stretching
1735 s	1732 s	C=O (ester) stretching
1711 s	1712 s	C=O (acid) stretching
	1649 s	Amide I (C=O) stretching
1659 sh		C=C stretching
	1546 s	Amide II (N–H) bending
1463 m	1470 m, 1434 m	CH_3 asymmetric bending, CH_2 scissoring
1378 m		CH_3 umbrella mode
1182 m		C–O–C (ester) stretching
717 w	720 w	CH_2 rocking

vs (very strong), *s* (strong), *m* (medium), *w* (weak), *sh* (shoulder), *S* symmetric, *AS* asymmetric

Analyses of oil paint reconstructions

Table 3 summarises the results achieved with surface ATR measurements performed on different oil paint reconstructions.

As it is already known that saponification can occur only if a Lewis base or acid is involved, the fact that organic-based pigments (indigo, carmine, madder and Indian yellow), chrome oxide, green earths, lapislazuli, artificial ultramarine, chalk, titanium white, Mars yellow, realgar, orpiment and lamp black did not show any production of metal carboxylates it is not surprising. Furthermore in these cases vibrational band occurrence and intensities of the linseed oil remained quite unchanged compared with the pure binding medium.

If compared with pure linseed oil spectrum (Fig. 4b), paint reconstructions made of cerulean blue and iron-based pigments, such as yellow and red ochre, Prussian blue and bole, showed a greater intensity of the free fatty acids band at 1710 cm^{-1} (Fig. 4a) relative to the ester one. This may suggest a key role possibly played by these pigments in promoting hydrolysis: these results merit further study which will be implemented by the authors.

On the surface of lead-based paint reconstructions the formation of lead carboxylates has been confirmed (Fig. 5) with the presence of stronger absorption intensities observed in litharge and red lead-based paints (Fig. 5c,d) compared with those observed on lead white (Fig. 5f). Lead carboxylates have been also detected on the grey paint reconstructions and this is obviously because they were prepared by mixing carbon-based pigments with lead white (Fig. 5e).

The free carboxylic acid band occurring at 1708–1719 cm^{-1} cannot be distinguished in litharge, red lead and grey paint reconstructions, whereas it presents an intensity that is almost of the same order of magnitude as that of the fatty ester in Naples yellow (Fig. 5a), lead tin yellow (Fig. 5b) and lead white paints (Fig. 5f). This could be an indication that, regardless of the fact that all these paints contain lead, the conversion into metal carboxylates of the free fatty acids produced by hydrolysis of the fatty esters did not occur at the same rate with all types of lead-based pigments. The free fatty acid band cannot be distinguished in the spectra collected from zinc white and cobalt green paints (Fig. 6). In this particular case the two spectra showed a similar profile with the presence of a broad band at about 1590 cm^{-1}. As both zinc white and cobalt green contain zinc oxide the presence of zinc soaps can be assumed even though the band does not correspond with that characteristic of the zinc palmitate (Fig. 2b). Nevertheless the band appears very broad and the presence of a mixture of carboxylates with different molecular weight, which includes zinc palmitate, can just be hypothesised.

Besides lead-based paints, other pigments gave rise to a partial formation of carboxylates as in the case of copper (malachite, azurite) (Fig. 7) and manganese-based paints (burnt and raw sienna, burnt and raw amber) (Fig. 8). The ATR spectra of copper-based paints show an absorption band at 1585 cm^{-1} (Fig. 7) which can be assigned to copper carboxylates as confirmed by the analogous band detected in the synthesised copper palmitate (Fig. 2c).

The interaction between an oil binding medium and manganese pigments has never been previously studied and the ATR measurements (Fig. 8) resulted in the identification of manganese carboxylates (bands at 1567 and 1545 cm^{-1}) (Fig. 2e,f) produced on burnt and raw sienna, and burnt and raw amber paint reconstructions. The key role played by

Table 3 Summary of metal carboxylates' occurrence on oil paint reconstructions

Oil paints	Metal involved	Carboxylates formation	Hydrolytic effects	Similar to pure linseed oil
Indigo				X
Carmine				X
Madder				X
Vine black				X
Lamp black				X
Orpiment	As			X
Realgar	As			X
Chalk	Ca			X
Ivory black	Ca			X
Cadmium red	Cd			X
Cadmium yellow	Cd	x		
Cobalt blue	Co			X
Cerulean blue	Co Sn		X	X
Chrome oxide	Cr			X
Emerald green	Cr			X
Azurite	Cu	x		
Malachite	Cu	x		
Veronese green	Cu	x		
Prussian blue	Fe		x	X
Red ochre	Fe		x	X
Yellow ochre	Fe		x	X
Bole	Fe Al		x	X
Mars yellow	Fe Al Ca			X
Green earth	Fe K Mg Al			X
Indian yellow	Mg			X
Burnt sienna	Mn Fe	x		
Burnt umber	Mn Fe Al	x		
Raw umber	Mn Fe Al	x		
Raw sienna	Mn Fe Al	x		
Lapislazuli	Na Al			X
Artificial ultramarine	Na Al			X
Red lead	Pb	x		
Litharge	Pb	x		
Lead white	Pb	x		
Vine black + lead white	Pb	x		
Lamp black + lead white	Pb	x		
Naples yellow	Pb Sb	x		
Lead tin yellow	Pb Sn	x		
Ivory black + lead white	Pb Ca	x		
Titanium white	Ti			X
Zinc white	Zn	x		
Cobalt green	Zn Co	X		

manganese metal ions, instead of the iron ones, in the production of metal carboxylates on these type of paint reconstructions can be inferred. This is confirmed by the fact that on iron-based paints, such as Prussian blue, bole, red and yellow ochre, the production of metal carboxylates has not been detected (Table 3).

Cadmium carboxylates (Fig. 2d) have been detected on cadmium yellow (CdS, cadmium sulphide) paint (Fig. 9a), whereas they were surprisingly absent on cadmium red paints (CdS·CdSe, cadmium sulphide selenide) (Fig. 9b). Particularly noteworthy is the production of copper carboxylates detected on the azurite [$2CuCO_3{\cdot}Cu(OH)_2$] paints (Fig. 7) where, in some areas of the paint reconstruction, the azurite pigment has been pseudomorfically replaced by malachite [$CuCO_3{\cdot}Cu(OH)_2$] (Fig. 7b) [21]. This finding, which is thought to be caused by an increasing moisture and carbon dioxide concentration of the surrounding environment, according to the following reaction,

$$2\left(2CuCO_3 \cdot Cu(OH)_2\right)+H_2O \rightleftharpoons 3\left(CuCO_3 \cdot Cu(OH)_2\right)+CO_2$$

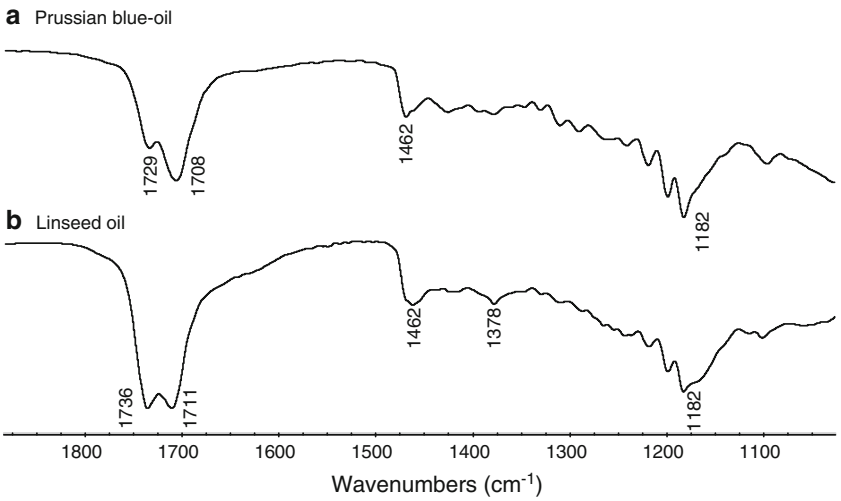

Fig. 4 ATR spectra of oil paint reconstructions of **a** Prussian blue and **b** standard linseed oil film

seems to be also associated with the contemporary presence of copper carboxylates into the converted areas.

The azurite paint reconstruction was first submitted to single-point micro ATR analyses which allowed the surface identification of azurite, malachite and copper carboxylates (Fig. 7). The resulting ATR mapping performed on a representative area of the blue paint (350 μm × 400 μm) (Fig. 10a) allowed a better localisation of the different components. Azurite and malachite were spatially localised by performing a peak area map of the O–H bending vibration at 946 cm^{-1} (Fig. 10b) and 1046 cm^{-1} (Fig. 10c), respectively. The peak at 1585 cm^{-1} was used for the mapping of the copper carboxylates (Fig. 10d). The FTIR false colour plots clearly indicate how the localisation of the copper carboxylates corresponds to that of malachite. Their concentration seems to be higher on these degraded areas than was observed on malachite paint reconstructions. This can be an indication that the conversion of azurite into malachite and the contemporary formation of hydrophilic copper carboxylates, localised in the same area, could be correlated. This particular aspect is still under investigation and will be subjected to further research.

Analyses of egg tempera paint reconstruction

Table 4 summarises the results achieved with surface ATR measurements performed on different egg tempera paint reconstructions in terms of formation of metal carboxylates on their surfaces. Due to the fact that the amide II band (1545 cm^{-1}), characteristic of any protein-based binding medium, absorbs in the same infrared spectral region of metal carboxylates, their presence cannot be ascertained unambiguously. On the other hand, apart from those metal carboxylates which show characteristic bands at frequencies higher or lower than 1545 cm^{-1}, their possible presence

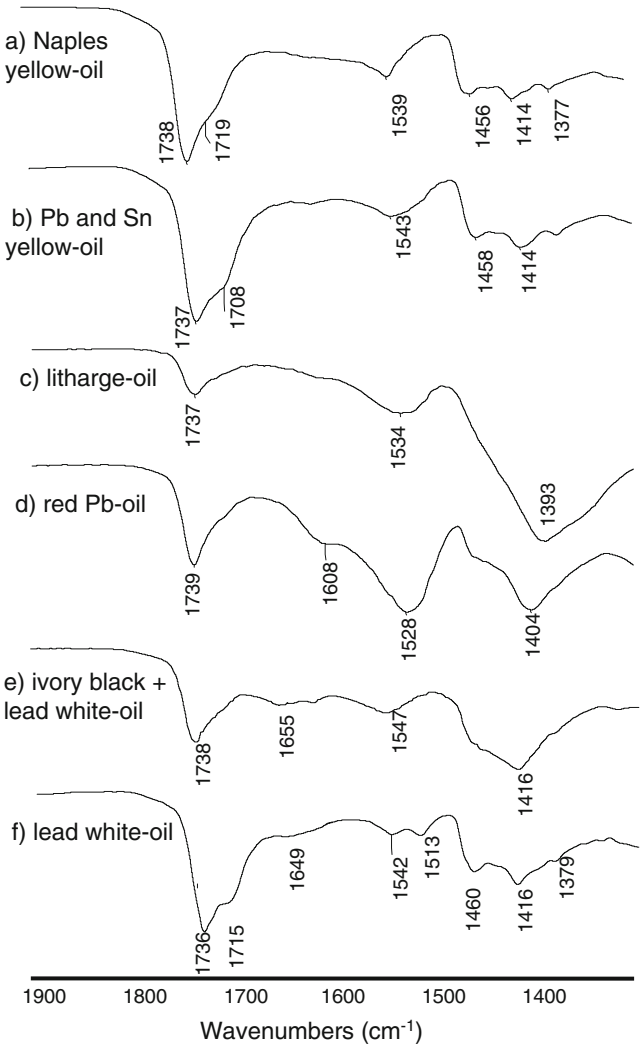

Fig. 5 ATR spectra of oil paint reconstructions of **a** Naples yellow, **b** lead tin yellow, **c** litharge, **d** red lead, **e** grey (ivory black + lead white) and **f** lead white

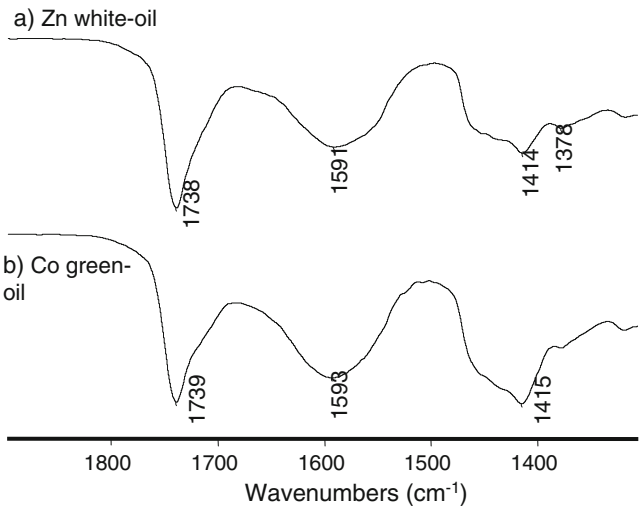

Fig. 6 ATR spectra of oil paint reconstructions of **a** zinc white and **b** cobalt green

can be deducted by taking into account the decrease in the value of the ratio between the transmittance percentage of amide II and amide I bands that, several measurements carried out on aged egg tempera films, showed to be higher than 1, owing to the fact that the amide II band always shows higher transmittance intensity values than the amide I (Fig. 3). Therefore, amide II/amide I values lower than 1 should account for a contribution belonging to the presence of metal carboxylates.

Among the analysed paint reconstructions a positive indication of the presence of metal carboxylates has been found on lead white, zinc white and azurite (Fig. 11a–c). The last of these, in spite of an amide II/amide I ratio value higher than 1, showed a distinctive peak at 1585 cm^{-1} assignable to copper palmitate (Fig. 2c). As far as the green

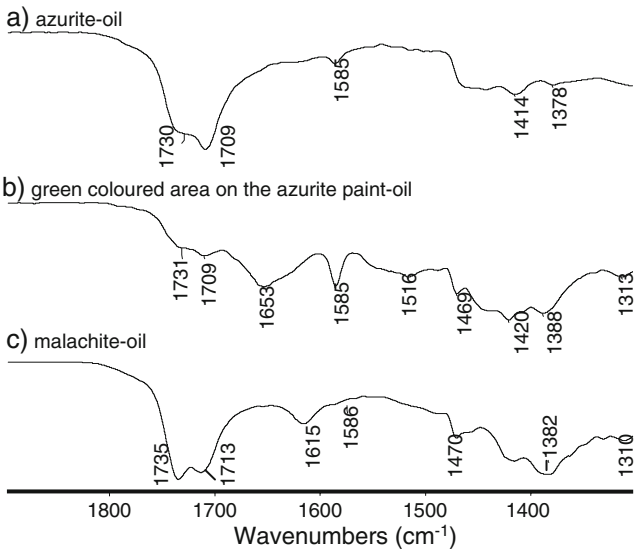

Fig. 7 ATR spectra of oil paint reconstructions of **a** azurite, **b** green-coloured area on the azurite paint and **c** malachite

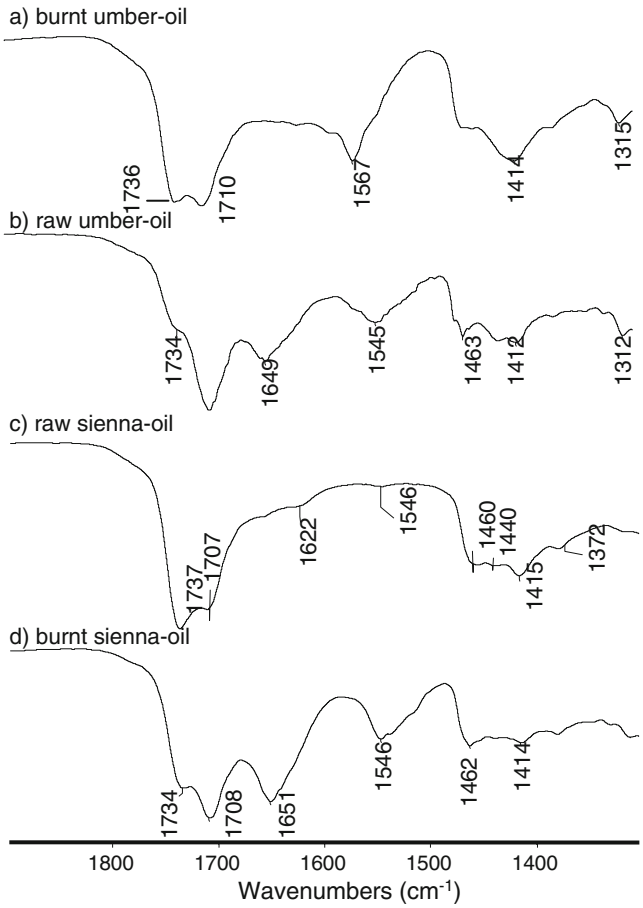

Fig. 8 ATR spectra of oil paint reconstructions of **a** burnt umber, **b** raw umber, **c** raw sienna and **d** burnt sienna

paints are concerned metal carboxylates have been detected only on malachite (Fig. 11d), which shows a distinctive peak at 1585 cm^{-1} (Fig. 2c) and cobalt green (Fig. 11e), where a peak at 1537 cm^{-1} assignable to Zn carboxylate is present (Fig. 2b).

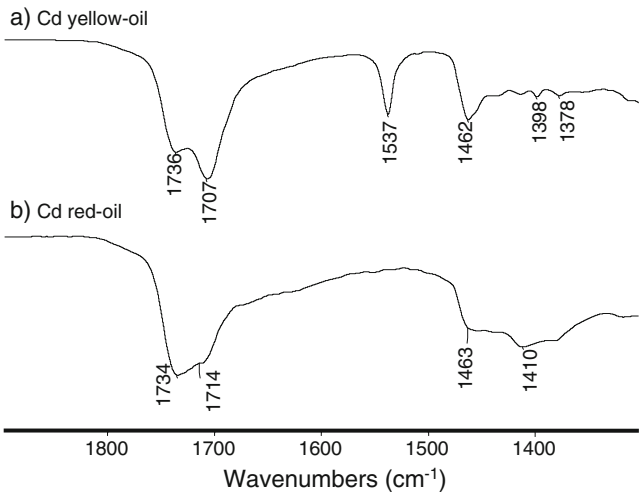

Fig. 9 ATR spectra of oil paint reconstructions of **a** cadmium yellow and **b** cadmium red

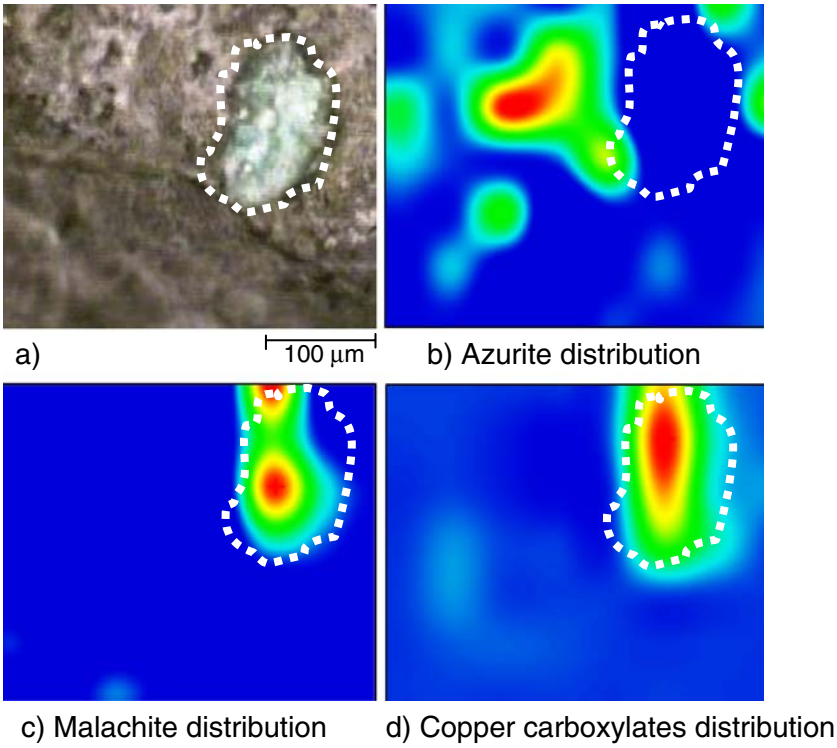

Fig. 10 FTIR false colour plots of the different paint components identified on a selected area of the azurite oil paint reconstruction. **a** Optical image of the mapped area; the *dotted line* represents the area where malachite and copper carboxylates coexist. **b** Distribution of the 946-cm^{-1} band of azurite. **c** Distribution of the 1046-cm^{-1} band of malachite. **c** Distribution of the 1585-cm^{-1} band of copper carboxylates

Table 4 Summary of metal carboxylates' occurrence on egg tempera paint reconstructions

Oil paints	Metal involved	Presence of carboxylates	Absence of carboxylates
Orpiment	As		X
Realgar	As		X
Chalk	Ca		X
Cadmium yellow	Cd	X	
Cobalt blue	Co		X
Chrome oxide	Cr		X
Emerald green	Cr		X
Azurite	Cu	X	
Malachite	Cu	X	
Yellow ochre	Fe		X
Bole	Fe Al		X
Mars yellow	Fe Al Ca		X
Indian yellow	Mg		X
Burnt umber	Mn Fe Mn Al	X	
Raw umber	Mn Fe Mn Al	X	
Raw sienna	Mn Fe Mn Al	X	
Lapislazuli	Na Al		X
Artificial ultramarine	Na Al		X
Red lead	Pb	X	X
Litharge	Pb	X	
Lead white	Pb	X	
Naples yellow	Pb Sb	X	
Lead tin yellow	Pb Sn	X	
Titanium white	Ti		X
Zinc white	Zn	X	
Cobalt green	Zn Co	X	

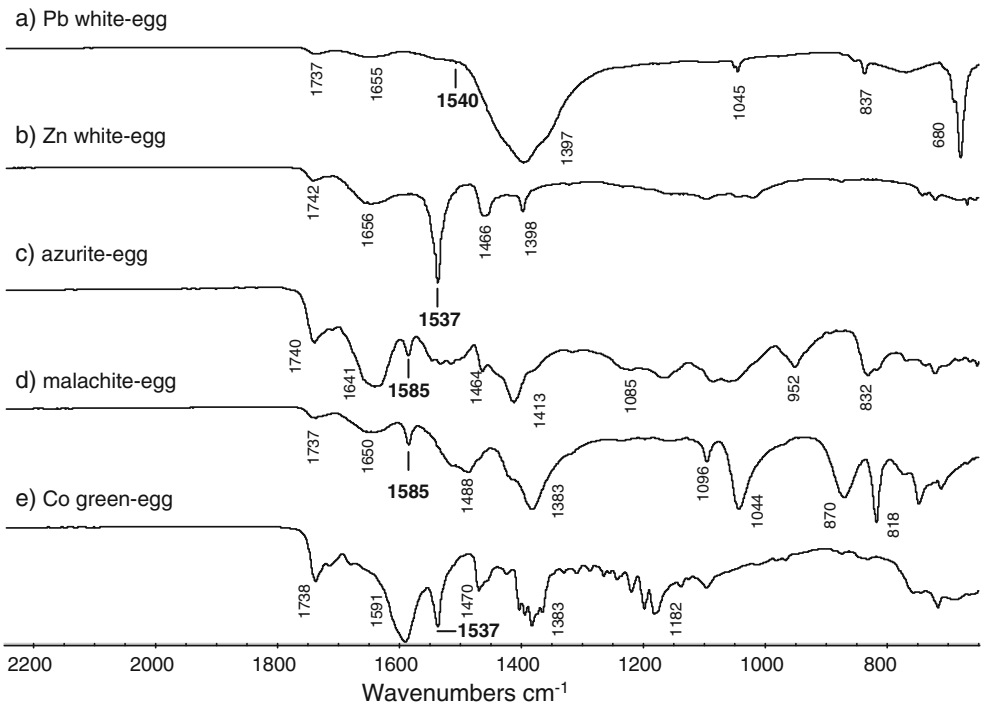

Fig. 11 ATR spectra of egg tempera paint reconstructions of **a** lead white, **b** zinc white, **c** azurite, **d** malachite and **e** cobalt green

Among the yellow paint reconstructions cadmium, Naples and lead tin yellows showed amide II/amide I values lower than 1 with additional sharp peaks at 1540 cm^{-1} (Fig. 2d) and 1512 cm^{-1} (Fig. 2a) assignable to Cd and Pb carboxylates, respectively. Litharge paints (Fig. 12) resulted in the formation of lead carboxylates and lead carbonate which showed distinctive peaks at 1400, 1044, 843 and 682 cm^{-1} (Fig. 12d). Analogous results have been obtained on red paints based on red lead (Fig. 12b) which were characterised by a sharp peak at 1514 cm^{-1} and lead carbonate formation. Among the other analysed red paints only raw and burnt umber showed the formation of metal carboxylates with an additional sharp peak at 1570 cm^{-1} assignable to Mn carboxylates (Fig. 2e,f).

The formation of lead carbonate on litharge and red lead paints (Fig. 12a,b) may be the result of degradation phenomena that have also been observed on oil-based litharge paints (Fig. 12c). This is certainly an issue which

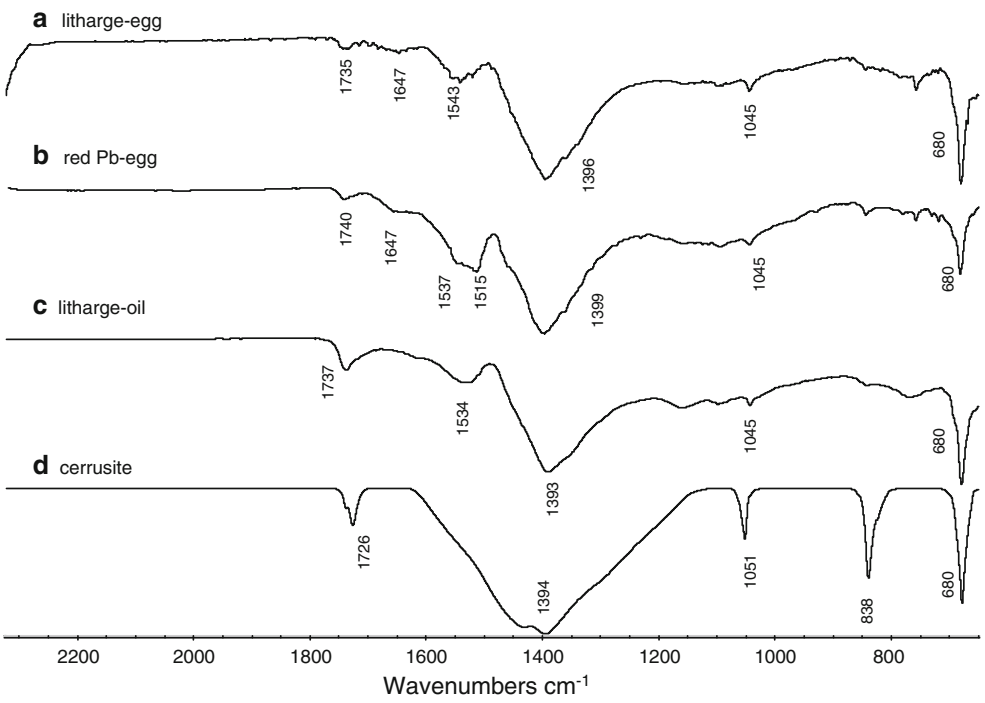

Fig. 12 ATR spectra of paint reconstruction made of **a** litharge egg tempera, **b** red lead egg tempera, **c** litharge oil paint and **d** reference lead carbonate (cerussite)

needs further confirmation even though it is known that organic components, such as acetic acid, act harshly upon lead and transform it into lead carbonate—as the museum objects conservation community is well aware of [22]. Acetic acid and some other acids, in the presence of carbon dioxide, react with lead to produce lead acetate and lead hydroxide that, in the presence of further carbon dioxide, form lead carbonate. Furthermore, both litharge and red lead are known to be highly reactive with siccative oil and, after just 80 days, the lead concentration in the oil is almost 13% in the case of litharge and 1.7% with red lead [23]. This may account for the reduced extent in which red lead oil and egg tempera paints were transformed into lead carbonate.

Conclusions

The use of micro ATR analyses allowed the study and the characterisation of metal carboxylates formed through the interaction between pigments and binding media of historically accurate reconstructions of oil and egg tempera composites naturally aged for 10 years. The synthesis of standard metal palmitates and the recording of their ATR spectra, with particular reference to manganese and cadmium palmitates, which were not available in the scientific literature, was deemed necessary in order to help the identification of metal soaps produced on the surface of the paint reconstructions. Among the different lead-based pigments, red lead and litharge seemed to produce a larger amount of carboxylates compared with lead white, Naples yellow and lead tin yellow. A possible degradation phenomenon which led to formation of lead carbonate has been observed on litharge and red lead paint dispersed in both oil and egg tempera binding media.

The formation of metal soaps was confirmed on both oil and egg tempera paints based on zinc, manganese and copper. On the last of these in particular, ATR mapping made it possible to spatially locate the areas where copper carboxylates were present and resulted in the observation that they coincided with the areas in which azurite has been pseudomorfically replaced by malachite. This may indicate a key role played by copper carboxylates in the conversion of azurite into malachite.

Most of the spectra collected from those iron-based paints which did not give rise to the production of metal soaps (yellow and red ochres, bole and Prussian blue) showed a more intense free fatty acid band compared with that of the reference siccative oil. This may suggest a role played by these type of pigments in the hydrolysis reaction pathway of the triglycerides and will be further researched. Furthermore, the key role played by manganese in the production of metals soaps on burnt and raw sienna and burnt and raw umber paints has been observed for the first time.

The formation of copper, lead, manganese, cadmium and zinc metal soaps was also identified on egg tempera paint reconstructions even though, in this case, the overlapping of the spectral region of the amide II band with that of metal carboxylates made their identification difficult.

References

1. Chiavari G, Fabbri D, Prati S (2005) J Anal Appl Pyrol 74:39–44
2. Adelantado JV, Mateo-Castro R, Domenech-Carbò MT, Bosch-Reig F, Domenech-Carbò A, Casas-Catalan MJ, Osete-Cortina L (2001) J Chromatogr A 922:385–390
3. Colombini MP, Modugno F, Giacomelli A (1999) J Chromatogr A 846:101–111
4. van der Weerd J (2002) Imaging microspectroscopic FTIR and VIS analysis of paint cross-sections. PhD dissertation, Amsterdam
5. Mills JS (1966) Studies Conserv 11:92–107
6. Robinet L, Corbeil MC (2003) Stud Conserv 48:23–40
7. O'Neill LA, Brett RA (1969) J Oil Col Chem Ass 52:1054–1074
8. Bell SH (1970) Paint Varnish Prod 60:55–60
9. Plater MJ, De Silva B, Gelbrich T, Hursthouse MB, Higgitt CL, Saunders DR (2003) Polyhedron 22:3171–3179
10. Keune K, Noble P, Boon JJ (2002) Proceedings of Art 2002, Antwerp, University of Antwerp, 2–6 June 2002
11. Keune K, Boon JJ (2004) Anal Chem 76:1374–1385
12. Keune K (2005) Binding medium, pigments and metal soaps characterised and localised in paint cross-sections. PhD dissertation, University of Amsterdam, 22 June 2005 (available online)
13. Zeidler G, Hesse H (1940) Paint Varnish Prod Manag 20:32–43
14. Cotte M, Checroun E, Susini J, Walter P (2007) Appl Phys A 89:841–848
15. Mazzeo R, Joseph E (2007) Eur J Mineral 17:1–9
16. Aldrovandi A, Altamura ML, Cianfanelli MT, Ritano P (1996) I quaderni di OPD 8:191–209
17. Kambe H (1961) Bull Chem Soc Jpn 34:1790–1793
18. Thompson DV Jr (trans) (1954) The craftsman's handbook: Il libro dell'arte by Cennino d'Andrea Cennini. Dover, New York
19. O'Neil LA (1963) Paint Technol 27:44–47
20. Meilunas R, Bentsen JG, Steinberg A (1990) Stud Conserv 35:33–51
21. Gettens RJ, West Fitzhung E (1997) Azurite and blueverditer. In: Roy A (ed) Artists' pigments 2. Oxford University Press, New York
22. Oddy WA (1975) The corrosion of metals on display. In: Conservation in archaeology and the arts. In: Brommelle NS, Smith P (eds) London: International Institute for Conservation of Historic and Artistic Works, pp 235–237
23. Shaeffer JA (1933) Official Digest Federation Paint Varnish Prod Club 126:180–189